Spinal 5-HT_{1A}R contributes to the analgesia of acupoint catgut embedding by inhibiting phosphorylation of the NMDA receptor GluN1 subunit in CFA-induced inflammatory pain in rats

Wen-Qiang Cui , Wen-Shan Sun , Fei Xu , Xue-Ming Hu , Wei Yang , Yang Zhou , Li-Xia Du , Wen-Wen Zhang , Qi-Liang Mao-Ying , Wen-Li Mi , Yu-Xia Chu , Yan-Qing Wang

PII: S1526-5900(18)30403-6
DOI: https://doi.org/10.1016/j.jpain.2018.07.011
Reference: YJPAI 3618

To appear in: *Journal of Pain*

Received date: 9 May 2018
Revised date: 21 July 2018
Accepted date: 24 July 2018

Please cite this article as: Wen-Qiang Cui , Wen-Shan Sun , Fei Xu , Xue-Ming Hu , Wei Yang , Yang Zhou , Li-Xia Du , Wen-Wen Zhang , Qi-Liang Mao-Ying , Wen-Li Mi , Yu-Xia Chu , Yan-Qing Wang , Spinal 5-HT_{1A}R contributes to the analgesia of acupoint catgut embedding by inhibiting phosphorylation of the NMDA receptor GluN1 subunit in CFA-induced inflammatory pain in rats, *Journal of Pain* (2018), doi: https://doi.org/10.1016/j.jpain.2018.07.011

Highlights

- Acupoint catgut embedding (ACE) attenuates the CFA–induced nocifensive response
- ACE and EA have similar effects but different characteristics in CFA rats
- Spinal 5-HT_{1A}R-GluN1-Ca^{2+}-dependent signaling cascades is involved in ACE analgesia

Title page

Spinal 5-HT_{1A}R contributes to the analgesia of acupoint catgut embedding by inhibiting phosphorylation of the NMDA receptor GluN1 subunit in CFA-induced inflammatory pain in rats

Wen-Qiang Cui[a,b,c,1], Wen-Shan Sun[d,1], Fei Xu[c,e], Xue-Ming Hu[a,b,c], Wei Yang[a,b,c], Yang Zhou[a,b,c], Li-Xia Du[a,b,c], Wen-Wen Zhang[a,b,c], Qi-Liang Mao-Ying[a,b,c], Wen-Li Mi[a,b,c], Yu-Xia Chu[a,b,c*], Yan-Qing Wang[a,b,c*]

[a] Department of Integrative Medicine and Neurobiology, School of Basic Medical Sciences, Fudan University, Shanghai, China

[b] Institutes of Brain Science, Brain Science Collaborative Innovation Center, State Key Laboratory of Medical Neurobiology, Fudan University, Shanghai, China

[c] The Institute of Integrative Medicine, Fudan University, Shanghai, China

[d] Department of Traditional Chinese Medicine, The Fifth People's Hospital of Shanghai, Fudan University, Shanghai, China

[e] Department of Integrative Medicine, Huashan Hospital, Fudan University, Shanghai, China

[1.] These authors contributed equally to this work.

[*] Corresponding author: Yu-Xia Chu, PhD or Yan-Qing Wang, PhD,
130 Dong'an Road, Shanghai 200032, China; yuxiachu@fudan.edu.cn (Yu-Xia Chu) or wangyanqing@shmu.edu.cn (Yan-Qing Wang).

Authors' contributions

Study design/planning: W.-S. S., Y.-Q. W., Y.-X. C., W.-Q. C., X.-M. H., W.-W. Z.

Study conduct: W.-Q. C., F. X., X.-M. H., Y. Z., L.-X. D., W. Y.

Technical guidance: W.-S. S.

Data analysis: W.-Q. C., F. X., X.-M. H.

Writing paper: W.-Q. C., Y.-Q. W., Y.-X. C, W.-S. S., F. X., X.-M. H., W.-W. Z

Revising paper: all authors

Authors' e-mail

Wen-Qiang Cui: 16111010087@fudan.edu.cn

Wen-Shan Sun: swensun@126.com

Fei Xu: xufeigaomi@163.com

Xue-Ming Hu: 15111520028@fudan.edu.cn

Wei Yang: 16211010079@fudan.edu.cn

Yang Zhou: 13111520014@fudan.edu.cn

Li-Xia Du: 15211010072@fudan.edu.cn

Wen-Wen Zhang: 17211010072@fudan.edu.cn

Qi-Liang Mao-Ying: maoyql@fudan.edu.cn

Wen-Li Mi: wenlimi@fudan.edu.cn

Yu-Xia Chu: yuxiachu@fudan.edu.cn

Yan-Qing Wang: wangyanqing@shmu.edu.cn

Corresponding author

Yan-Qing Wang, PhD

Department of Integrative Medicine and Neurobiology, School of Basic Medical Sciences, Fudan University.

Mailing address: 130 Dong'an Road, Xuhui District, Shanghai 200032, P.R.CHINA.

E-mail: wangyanqing@shmu.edu.cn

Telephone number: +86-21-54237496

Fax: 86-21-54237611

Disclosures

This study was financially supported by the National Key R&D Program of China (2017YFB0403803), the National Natural Science Funds of China (31600852, 81473749, 81771202), and the Development Project of Shanghai Peak Disciplines-Integrated Chinese and Western Medicine.

The authors declare that there are no conflicts of interest regarding the publication of this paper.

Abstract

Acupoint catgut embedding (ACE) is a widely used traditional Chinese medicine method to manage various diseases, including chronic inflammatory pain. We sought to assess the possible analgesic effects of ACE in comparison to electroacupuncture (EA) and to study the analgesic mechanisms of ACE in a rat model of inflammatory pain induced by injection of complete Freund's adjuvant (CFA) into the hind paw of rats. The von Frey, radiant heat, and gait analysis tests were performed to evaluate the analgesic effects of ACE and EA, and western blot and immunohistochemistry assays were carried out to determine the molecular mechanisms of ACE. ACE treatments were administered every four days or every week with different acupoints (ipsilateral, contralateral, or bilateral ST36 and GB30 acupoints). The most effective ACE strategy for attenuating the nocifensive response induced by CFA injection was performing ACE once a week at ipsilateral ST36 in combination with GB30. EA treatment every other day at ipsilateral ST36 and GB30 showed comparable analgesic effects. ACE inhibited the increased activation of the GluN1 subunit of the NMDA receptor and the subsequent Ca^{2+}-dependent signals (CaMKII, ERK and CREB) that take place in response to CFA. The effects of ACE were similar to intrathecal injection of vilazodone (a 5-HT_{1A}R agonist) and were blocked by WAY-100635 (a 5-HT_{1A}R antagonist). In summary, we show that ACE attenuates CFA-induced inflammatory pain in rats by activating spinal 5-HT_{1A}R and by inhibiting the phosphorylation of GluN1 and thus inhibiting the activation of Ca^{2+}-dependent signaling cascades.

Perspective

This article presents the novel evidence concerning the spinal 5-HT_{1A}R activation-related molecular signaling of ACE analgesia in a rat model of CFA-induced inflammatory pain. This work may help the clinicians to verify the effectiveness of ACE analgesia and to better understand the underlying mechanism.

Keywords

Acupoint stimulation; Electroacupuncture; Serotonin; Ca^{2+}-dependent signal cascade; Spinal cord.

Introduction

Acupuncture, which can be performed in several different ways, has been widely used for managing many diseases, including chronic inflammatory pain, especially in drug-refractory patients [3, 4, 55]. Several large studies have also provided evidence that acupuncture is a relatively safe treatment [34, 47, 50].

Acupoint catgut embedding (ACE) refers to injecting sutures made of absorbable materials at acupoints that are associated with different physiological processes or diseases. This is a combination of ancient traditional acupuncture and modern tissue therapy [11, 42, 43], and as a variant of acupuncture, it has been practiced along with traditional acupuncture in China for thousands of years. ACE stimulates the acupoint persistently for a week or longer until the suture undergoes softening, liquefaction, and absorption [11]. Therefore, ACE is more convenient than traditional acupuncture, which needs to be performed daily or every other day. Moreover, ACE is easier to perform than traditional acupuncture and is thus widely used to treat various disorders in China such as obesity [18], allergic rhinitis [28], etc. In particular, it has been widely used to manage clinical pain [13, 31, 51]. However, the mechanisms behind ACE's analgesic effects remain unclear. Thus, establishing an animal model to study its analgesic mechanisms and to popularize its application is meaningful.

ACE generates mild and long-lasting stimulation at specific acupoints through the injection of catgut, which is similar in essence to electroacupuncture (EA). Therefore, it has been speculated that ACE might share some common mechanisms with EA analgesia [18, 28]. Previous research suggests that the activation of serotonergic inhibition on the activities of spinal neurons is at least partly behind the analgesic effects of EA [26, 53, 57]. Moreover, 5-HT_{1A}R, which is a subtype of the 5-HT receptors, plays an important role in serotonergic-mediated effects on the nervous system, and inhibition of 5-HT_{1A}R prevents the analgesic effects of EA in a collagen-induced arthritis pain model [2]. Previous studies also showed that spinal 5-HT_{1A}R and the GluN1 subunit of the N-methyl-D-aspartate (NMDA) receptor are involved in acupuncture's analgesic effects in a complete Freund's adjuvant (CFA)-induced inflammatory pain model [54] and that 5-HT_{1A}R activation prevents the phosphorylation of GluN1 [37], which plays an important role in the regulation of the Ca^{2+}-dependent signal cascade through the phosphorylation of CaMKII, ERK,

and CREB [29, 49].

Thus, we hypothesized that spinal 5-HT_{1A}R, GluN1, and the Ca^{2+}-dependent signaling cascade are all involved in ACE analgesia. In the present study, we found that ACE showed long-lasting analgesic effects in the CFA models similar to the effects of EA and that blocking 5-HT_{1A}R activity markedly reduced the analgesic effects of ACE. Moreover, the decreased phosphorylation of the GluN1 subunit of the NMDA receptor and subsequent decrease in phosphorylation of CaMKII, ERK, and CREB were involved in the 5-HT_{1A}R-mediated analgesic effect of ACE.

Materials and methods

Animals

The experiments were performed on adult male Sprague-Dawley rats weighing 200–300 g. The rats were supplied by the Experimental Animal Center, Chinese Academy of Sciences, Shanghai, China. The rats were maintained under constant conditions (22–24°C and 12 h light-dark cycle) with food and water available ad libitum. Four animals were housed per cage and allowed to acclimate to these conditions for at least 1 week before inclusion in the experiments. All animal procedures in this study were conducted in strict accordance with the NIH Guide for the Care and Use of Laboratory Animals and the ethical standards of the International Association for the Study of Pain [59]. Best efforts were exerted to minimize both the number of animals used and their suffering. For each experiment, the animals were randomly divided into groups. The sample size was calculated based on our previous work.

Induction of inflammatory pain

To induce inflammatory pain, CFA (Sigma, suspended in an 1: 1 oil/saline emulsion, 0.1 ml, 50 μg Mycobacterium tuberculosis) was subcutaneously injected into the right hind paw of the rats using a 500 μL BD syringe with a 30 1/2-gauge needle. Saline (0.9%, 0.1 ml) was used for the vehicle control group. Except for measuring the time course of CFA-induced inflammatory pain, all other experiments were performed 1–15 days after saline or CFA injection when the tissue inflammation in the hind paws was obvious, including erythema, edema, and hyperpathia.

Behavioral studies

Mechanical allodynia was measured with a series of von Frey hairs (0.4, 0.6, 1.4, 2.0, 4.0, 6.0,

8.0, and 15.0 g) (Stoelting, USA) according to the up-and-down method described in a previous study [33]. Briefly, the rats were placed individually into a Plexiglas cage with a wire net floor and allowed to acclimate for 15–20 min. The animals were acclimated to this environment for 2–3 days by recording a series of baseline measurements. The von Frey hairs were held against the skin for about 6–7 seconds with a 10 min interval between applications. A trial began with the application of the 2.0 g hair. A positive response was defined as the brisk withdrawal of the hind paw upon stimulation. When there was a positive response to a hair, the smaller hair was used next; when there was a negative response, the larger hair was used next. Five more stimulations were administrated after the first positive response was observed. The final score was converted to a 50% paw-withdrawal threshold (PWT) using an adaptation of the Dixon up-down paradigm as previously described [33].

Thermal hyperalgesia was reflected by the paw-withdrawal latency (PWL) to radiant heat. The PWL was measured by using an IITC Model 390 Paw Stimulator Analgesia Meter (Life Science Instruments, USA) as previously described [21]. The rats were allowed to acclimate to the environment for 15–20 min in a Plexiglas cage set upon the elevated special diabatic glass. Radiant heat was applied to irradiate the plantar surface of each paw until the rat lifted its paw from the glass. The intensity of radiant heat was adjusted to elicit the response at around 12–14 s in control rats, and the heat was maintained at a constant intensity. A 20 s cut-off time and a 10 min interval between trials were imposed to avoid tissue damage. Five trials were administrated for each rat. The longest and shortest times were removed, and the average of the three remaining data points was calculated. The mean time from beginning of the heating to the lifting of the rat's hind paw was defined as the PWL.

The changes in gait after CFA injection and ACE treatment were analyzed with the CatWalk Analysis System (Noldus Information Technology, Wageningen, The Netherlands) as previously described [19]. Briefly, this test was conducted in a dark and silent room. The rat was placed on a 1.5 m enclosed glass plate with a light beam from a fluorescent lamp projecting through the glass plate, and the rat was tempted by food to travel across the plate. A high-speed camera was placed under the plate with a focal length that allowed it to capture more than three complete gaits when the rat walked through the filming region. Each rat was tested at least three times, and the gait parameters were analyzed using the CatWalk Analysis software (CatWalk XT 10.0). Gait

parameters were automatically labeled as right forepaw, right hind paw, left forepaw, and left hind paw, and six spatiotemporal parameters, including max contact area (the area contacted at the moment of maximum paw-floor contact during stance phase), mean contact area (the mean contact area of the complete paw), max contact max intensity (the max intensity of a paw at the moment of maximal paw-floor contact), mean intensity (the mean intensity of the complete paw), swing time (the duration of no contact between a paw with the glass CatWalk plate), and stand time (the duration in seconds of contact of a paw with the glass), were incorporated in our results to evaluate the motor function of the animals. The first four values were adjusted by the ratio of the affected side (right hind paw) to the unaffected side (left hind paw).

EA and ACE treatment

EA treatment started on day 1 after CFA injection. Before EA, the rats were bound by a tailored apparatus so that their bodies were held still while their heads and four limbs could move freely. The rats were allowed to acclimate to this for 20 min and then a pair of stainless steel acupuncture needles (diameter 0.3 mm) were inserted vertically into the ipsilateral (right side) acupoint "Zusanli" (ST36, 5 mm below the anterior tubercle of tibia, and 2 mm lateral to the knee joint; the lateral sural cutaneous nerve and the cutaneous branch of the saphenous nerve) and "huantiao" (GB30, the posterosuperior border of the hip joint of the hind limbs; underneath are the sciatic nerve, inferior gluteal nerve, and gluteal muscles) at a depth of 6 mm. To keep a consistent and reproducible depth, the needles were bent into an 'L' shape. The handles of these needles were connected to the output terminals of a HANS Acupuncture Point Nerve Stimulator (LH-202H Huawei Co., Ltd., Beijing, China). Parameters of EA were as follow: square wave output current (pulse width: 0.2 ms), 3-4 mA (each current intensity for 15 min), and alternating dense–sparse frequencies (alternating between 100 Hz for 3s and 2 Hz for 3s). Sham EA rats received the same treatment but without electrical stimulation.

ACE treatment was administered from day 1 post-CFA. A disposable catgut embedding needle (diameter 0.7 mm; Gaoguan Medical, Zhenjiang, China) (**Fig. 1A**) and absorbable catgut (0.5 cm length (as determined by preliminary experiments); collagen wire, 2-0, 2 cm*10, BD150101, Boda Co., Ltd., Shandong, China) (**Fig. 1B**) were used in our studies. The rats in the ACE treatment group were anesthetized with isoflurane (2% in a 1:1 mixture of oxygen and air, RWD Life Science Co., Shenzhen, China), and the absorbable catgut was implanted into ST36 and GB30 at a

depth of 0.3 cm using the embedding needle (**Fig. 1C**). Sham ACE rats received the same treatment but without catgut injection.

Drug administration

Vilazodone (a partially selective 5-HT_{1A}R agonist, Selleck, USA) and WAY-100635 (a selective 5-HT_{1A} antagonist, Selleck, USA) were delivered intrathecally using a method of lumbar puncture, which was performed using a 10 μl microsyringe as previously described [23]. The needle was inserted into the intervertebral space between the L5–6 interspace of the spinal cord after the rat was anesthetized with isoflurane aerosol. The accuracy of each injection was indicated by a tail-flick or paw-flick response. The administration time and dosage were determined by preliminary experiments.

Western blot analysis

To measure the protein level of p-ERK, the sampling method was adjusted on the basis of the previously described method [7]. On the day of the experiments, the rat was anesthetized with sodium pentobarbital (50 mg/kg, intraperitoneal). Subsequently, the right hind paw of all groups was mechanically stimulated by repeated flexion and extension of the ankle joint for 2 min within the normal physiological working range of the joint. The L4-6 segments of the spinal cord were quickly removed and ultrasonically disrupted in radioimmunoprecipitation assay (RIPA) lysis buffer (50 mM Tris (pH 7.4), 150 mM NaCl, 1% Triton X-100, 1% sodium deoxycholate, 0.1% sodium dodecyl sulfonate, sodium orthovanadate, sodium fluoride, ethylenediaminetetraacetic acid, and leupeptin), followed by centrifugation at 12,000 × *g*. The total protein level in the supernatants was measured using the Pierce bicinchoninic acid (BCA) Protein Assay Kit (Thermo Scientific, Rockford, IL, USA). The protein samples were separated by 10% SDS-PAGE and then transferred onto polyvinylidene fluoride (PVDF) membranes. After blocking with 5% nonfat milk dissolved in 1% TBST (20 mM Tris–HCl, pH 7.5, 150 mM NaCl, and 0.05% Tween-20) for 1.5 h at room temperature, the membranes were probed with the following primary antibodies: rabbit anti-phosphorylated GluN1 (p-NR1, Ser897, 1:800 dilution, C05008H, Signalway Antibody, USA), rabbit anti-phosphorylated extracellular signal-regulated kinase (p-ERK, Thr202/Tyr204, 1:800 dilution, 4370, Cell Signaling Technology, Boston, MA, USA), rabbit anti-phosphorylated Ca(2+)/calmodulin-dependent protein kinase Ⅱ α (p-CaMKII, Thr286, 1:1000 dilution, SC-12886-R, Santa Cruz Biotechnology, Santa Cruz, CA, USA), rabbit anti-phosphorylated

cAMP response element binding protein (p-CREB, Ser133, 1:1000 dilution, 9198, Cell Signaling Technology), and HRP-conjugated mouse anti-GAPDH antibody (1:10,000 dilution, 51332, Proteintech, Manchester, UK) at 4°C overnight. The blots were washed in TBST and incubated with the HRP-conjugated goat anti-rabbit IgG (H+L) secondary antibody (1:10,000 dilution, MR-G100, MRBiotech, Shanghai, China) for 1–2 h at room temperature. Western blot images were captured on an ImageQuant LAS4000 mini image analyzer (GE Healthcare, Buckinghamshire, UK), and band intensities were quantified using the Quantity One Analysis Software (Version 4.6.2, Bio-Rad Laboratories, Hercules, USA). The protein band densities of p-GluN1, p-ERK, p-CaMKII, and p-CREB were normalized against the density of GAPDH. The fold change of the control group was set as 1 for quantifications.

Immunofluorescence

The rats were deeply anesthetized with sodium pentobarbital (50 mg/kg, intraperitoneal) and then intracardially perfused with saline followed by 4% paraformaldehyde (PFA). The L4 to L6 spinal segments were removed, postfixed in 4% PFA for 12 hours, and allowed to equilibrate in 30% sucrose in a phosphate buffer for 3–4 days at 4°C. The segments were imbedded and frozen in encompassing agent (Leica, Germany) and then sectioned on a freezing microtome (Leica 2000, Germany) at a thickness of 30 μm and processed for immunohistochemistry. After washing with PBST (phosphate-buffered saline with 0.3% Triton X-100) three times, the sections were blocked with 5% donkey serum for 1.5 h at room temperature then incubated overnight at 4°C with the following primary antibodies: rabbit anti-5-HT_{1A}R antibody (1:800 dilution, ab85615, Abcam, UK), goat anti-5-HT_{1A}R antibody (1:100 dilution, sc1459, Santa Cruz Biotechnology), mouse anti-NMDAR1 antibody (1:500 dilution, ab134308, Abcam), rabbit anti-phosphorylated GluN1 (p-NR1, Ser897, 1:500 dilution, ABN99, Millipore, USA), mouse anti-NeuN (neuronal marker; 1:500 dilution, MAB377, Millipore), rabbit anti-NeuN (1:500 dilution, ab177487, Abcam), rabbit anti-glial fibrillary acidic protein (anti-GFAP, astrocyte marker; 1:500 dilution, 12389, Cell Signaling Technology), mouse anti-GFAP (1:500 dilution, 3670, Cell Signaling Technology), and goat anti-Iba1 (microglial marker; 1:500 dilution, ab5076, Abcam). The sections were then washed with PBST three times and incubated with a mixture of Alexa 488-conjugated and Alexa 594-conjugated secondary antibodies (1:1,000 dilution, Invitrogen, USA) for 1 h at room temperature. All sections were washed three times and coverslipped with a mixture of 80%

glycerin in 0.01 M PBS. Finally, images were captured using a multiphoton laser point scanning confocal microscopy system (FV1000, Olympus, Tokyo, Japan).

Statistical analysis

The animal data are shown as the mean ± SEM (standard error of the mean). All statistical analyses were performed in GraphPad Prism 5 (GraphPad Software Inc., San Diego, CA, USA). The statistical significance of differences between groups was analyzed with Student's t-test or one-way analysis of variance (ANOVA) followed by a Dunnett multiple comparison test. Analysis of the time course of mechanical allodynia and thermal hyperalgesia was performed using two-way repeated-measures ANOVA followed by a Tukey's test. Pearson correlation was used for the linear correlation analysis. $P < 0.05$ was used as the threshold of significance in all analyses.

Results

The nocifensive response induced by CFA injection was attenuated by ACE treatments

We first established the CFA rat model. In the von Frey tests, the ipsilateral PWTs of the CFA rats were significantly decreased from the first day after CFA injection, and this effect lasted for at least 31 days after CFA injection (two-way ANOVA and Tukey's test, $F_{2,21} = 109.3$, $P < 0.0001$, **Fig. 2A**). In the radiant heat test, the CFA rats exhibited a significant decrease in PWLs over the same time frame (two-way ANOVA and Tukey's test, $F_{2,21} = 92.32$, $P < 0.0001$, **Fig. 2B**). These results indicated that the rats developed mechanical allodynia and thermal hyperalgesia after CFA injection.

To examine the role of ACE on CFA-induced nocifensive response, ACE was performed subcutaneously at different frequencies and different acupoints starting from 1 day after CFA injection. First, bilateral, ipsilateral, and contralateral (left side) ACE at ST36 and GB30 once a week demonstrated long-lasting analgesic effects on the mechanical allodynia (two-way ANOVA and Tukey's test, contralateral: $F_{3,28} = 66.86$, $P < 0.0001$, **Fig. 3A**; ipsilateral: $F_{3,28} = 41.18$, $P < 0.0001$, **Fig. 3B**; bilateral: $F_{3,28} = 59.16$, $P < 0.0001$, **Fig. 3C**) and thermal hyperalgesia (two-way ANOVA and Tukey's test, $F_{3,28} = 24.96$, $P < 0.0001$, **Fig. 3G**) induced by CFA, and no significant difference was seen compared to the frequency of once every 4 days (two-way ANOVA and Sidak's test, contralateral: $F_{1,14} = 0.1533$, $P = 0.7013$, **Fig. 3A**; ipsilateral: $F_{1,14} = 0.0451$, $P =$

0.8349, **Fig. 3B**; bilateral: $F_{1,14}$ = 0.0494, *P* = 0.8272, **Fig. 3C**; thermal hyperalgesia: $F_{1,14}$ = 0.0106, *P* = 0.9196, **Fig. 3G**). Therefore, once a week was used for the following experiments. It should be noted that the maximal analgesic effects occurred 3–4 days after each ACE treatment. Second, ipsilateral ACE showed approximately the same analgesic effects compared with bilateral application (two-way ANOVA and Sidak's test, mechanical allodynia ipsilateral vs. bilateral: $F_{1,14}$ = 0.7087, *P* = 0.4140, **Fig. 3E**; thermal hyperalgesia ipsilateral vs. bilateral: $F_{1,14}$ = 0.0023, *P* = 0.9622, **Fig. 3H**), while the analgesic effects of bilateral ACE were markedly superior to contralateral ACE (two-way ANOVA and Sidak's test, bilateral vs. contralateral: $F_{1,14}$ = 4.613 , *P* = 0.0496, **Fig. 3D**; ipsilateral vs. contralateral: $F_{1,14}$ = 0.2161, *P* = 0.6492, **Fig. 3F**). Therefore, to minimize injury to the animals, ipsilateral ACE was chosen over bilateral treatment. Third, ACE treatment had weak analgesic effects when it was applied at the ipsilateral ST36 or GB30 acupoints separately compared with performing ACE at both ST36 and GB30 simultaneously (two-way ANOVA and Sidak's test, mechanical allodynia ST36 vs. ST36 and GB30: $F_{1,14}$ = 0.9662 , *P* = 0.3423; mechanical allodynia GB30 vs. ST36 and GB30: $F_{1,14}$ = 11.24 , *P* = 0.0047; thermal hyperalgesia ST36 vs. ST36 and GB30: $F_{1,14}$ = 4.6052, *P* = 0.0499; thermal hyperalgesia GB30 vs. ST36 and GB30: $F_{1,14}$ = 10.96, *P* = 0.0052; **Fig. 4A and B**). Meanwhile, performing ACE at the ipsilateral ST25 and GB25 acupoints, which are commonly considered to be stomachache-related acupoints, had no analgesic effects (two-way ANOVA and Sidak's test, mechanical allodynia CFA+ST25+GB25 vs. CFA: $F_{1,14}$ = 0.02, *P* = 0.8897; thermal hyperalgesia CFA+ST25+GB25 vs. CFA: $F_{1,14}$ = 0.0811, *P* = 0.78; **Fig. 4A and B**). Thus, ipsilateral GB30 and ST36 ACE once a week was the most effective ACE strategy for attenuating the nocifensive response induced by CFA injection in our study.

To determine whether ACE has an effect on basal pain perception, the PWTs of naïve rats after ACE application was tested. ACE did not alter the PWTs of intact naïve rats (two-way ANOVA and Sidak's test, $F_{1,14}$ = 2.013, *P* = 0.1779, **Fig. S1**). Consistent with a previous study [11], ACE showed significant anti-edema effects in the CFA models (two-way ANOVA and Sidak's test, $F_{1,14}$ = 6.908, *P* = 0.0199, **Fig. S2**). However, it had no effect on the contralateral decreased PWTs induced by CFA injection (two-way ANOVA and Sidak's test, $F_{1,12}$ = 0.8169, *P* = 0.3839, **Fig. S3**). In addition, ACE had a week analgesic effect in a chronic constriction injury (CCI) model (two-way ANOVA and Sidak's test, $F_{1,14}$ = 4.736, *P* = 0.0471, **Fig. S4**), but no effect in spared

nerve injury (SNI) models (two-way ANOVA and Sidak's test, $F_{1,14}$ =2.798, P = 0.1165, **Fig. S5**).

Gait analysis is considered to be a method that effectively detects mechanical sensitivity related to the function of the hind limbs under conditions of chronic pain [14, 45], and we used the CatWalk gait analysis system to determine the effect of ACE on CFA-induced gait abnormalities. The max contact max intensity and the mean intensity of the ipsilateral hind paw were reduced at day 5 and day 11 after CFA injection (one-way ANOVA and Tukey's test, max contact max intensity day 5: F = 40.66, P < 0.0001; day 5 sham vs. CFA: P < 0.0001; max contact max intensity day 11: F = 21.61, P < 0.0001; day 11 sham vs. CFA: P < 0.0001; mean intensity day 5: F = 57.69, P < 0.0001; day 5 sham vs. CFA: P < 0.0001; mean intensity day 11: F = 27.44, P < 0.0001; day 1 sham vs. CFA: P < 0.0001; **Fig. 5E and F**), while max contact area and mean contact area did not change when the rat was walking (one-way ANOVA and Tukey's test, max contact area day 5: F = 0.0867, P = 0.9173; max contact area day 11: F = 0.1031, P = 0.9025; mean contact area day 5: F = 0.5134, P = 0.6058; mean contact area day 11: F = 1.137, P = 0.3398; **Fig. 5A-D**). The time of the standing phase was reduced at day 5 and day 11 after CFA injection (one-way ANOVA and Tukey's test, day 5: F = 39.64, P < 0.0001; day 5 sham vs. CFA: P < 0.0001; day 11: F = 39.14, P < 0.0001; day 11 sham vs. CFA: P < 0.0001; **Fig. 5G**), while the time of the swing phase significantly increased at day 5 after CFA injection (one-way ANOVA and Tukey's test, F = 25.12, P < 0.0001; sham vs. CFA: P < 0.0001; **Fig. 5H**) with a trend of increasing at day 11 after CFA injection (one-way ANOVA and Tukey's test, F = 3.182, P = 0.0621; sham vs. CFA: P = 0.0517; **Fig. 5H**). ACE was performed on day 1 and day 8 after CFA injection, and the gait analysis was performed at the maximal analgesic effects point, i.e. day 5 and day 11 after CFA injection. ACE increased the max contact max intensity and the mean intensity of CFA rats at day 5 and 11 after CFA injection (max contact max intensity day 5: CFA vs. CFA+ACE : P = 0.0037; max contact max intensity day 11: CFA vs. CFA+ACE : P = 0.0051; mean intensity day 5: CFA vs. CFA+ACE : P = 0.0001; mean intensity day 11: CFA vs. CFA+ACE : P = 0.0013; **Fig. 5E and F**). ACE increased the time of the standing phase at day 11 after CFA (CFA vs. CFA+ACE, P = 0.0117, **Fig. 5G**), but there was only an increased tendency at day 5 (CFA vs. CFA+ACE, P = 0.054, **Fig. 5G**). ACE caused a weak decrease in the time of the swing phase at days 5 (CFA vs. CFA+ACE, P = 0.0842) and 11 (CFA vs. CFA+ACE, P = 0.3032) after CFA, but the differences were not significant (**Fig. 5H**). These results showed that ACE

could alleviate the mechanical allodynia and thermal hyperalgesia and ameliorate the abnormal gait in CFA-induced inflammatory pain.

Both ACE and EA alleviated the mechanical allodynia and thermal hyperalgesia induced by CFA injection

A previous study reported that EA dramatically reduces mechanical allodynia and thermal hyperalgesia in CFA rats [46]. Our results showed that ACE has a remarkable analgesic effect on CFA-induced pain behaviors, so the analgesic effects and characteristics of these two alternative therapies (ACE and EA) were compared in our study. EA had immediate effects at 0–60 min after treatment, while ACE showed no immediate analgesic effects (two-way ANOVA and Tukey's test, PWT: $F_{5,42} = 54.66$, $P < 0.0001$, **Fig. 6A**; PWL: $F_{5,42} = 64.32$, $P < 0.0001$, **Fig. 6B**). Interestingly, a single ACE treatment produced a chronic analgesic effect that lasted for more than 7 days, but a single EA treatment did not (two-way ANOVA and Tukey's test, PWT: $F_{5,42} = 44.07$, $P < 0.0001$, **Fig. 6C**; PWL: $F_{5,42} = 31.62$, $P < 0.0001$, **Fig. 6D**). Notably, the mechanical allodynia and thermal hyperalgesia induced by CFA injection were largely inhibited by both repeated application of ACE (embedding catgut at the ipsilateral ST36 and GB30 acupoints once a week) and EA (inserting and stimulating needles at the ipsilateral ST36 and GB30 acupoints every two days) during the whole process (two-way ANOVA and Tukey's test, PWT: $F_{5,42} = 47.4$, $P < 0.0001$, **Fig. 6E**; PWL: $F_{5,42} = 20.8$, $P < 0.0001$, **Fig. 6F**). No significant differences were seen between the two treatments (two-way ANOVA and Sidak's test, PWT: $F_{1,14} = 0.0552$, $P = 0.8177$; PWL: $F_{1,14} = 0.0001$, $P = 0.9925$; **Fig. 6E and F**). These data indicated that both repeated ACE and EA have prolonged analgesic effects in CFA-induced inflammatory pain, although they showed different characteristics in terms of the timing and extent of their effects. Therefore, it is speculated that ACE and EA likely have some common mechanisms of action, but also some different mechanisms, in their analgesic effect on CFA-induced inflammatory pain.

Spinal 5-HT_{1A}R activation contributed to ACE analgesia in CFA-induced inflammatory pain

5-HT_{1A}R and GluN1 have previously been shown to be involved in EA-induced analgesia [54]. In order to study the roles of 5-HT_{1A}R on ACE's analgesia in CFA rats, a 5-HT_{1A}R partial agonist (vilazodone, a new antidepressant drug) and selective antagonist (WAY-100635) were injected intrathecally. Behavioral testing showed that vilazodone and WAY-100635 had no influence on the basal PWTs or PWLs of naïve rats (T test, PWT vilazodone: $P = 0.8285$, **Fig. 8A**; PWL

vilazodone: $P = 0.2894$, **Fig. 8B**; PWT WAY100635: $P = 0.5570$, **Fig. 7A**; PWL WAY100635: $P = 0.5498$, **Fig. 7B**). A single intrathecal injection of vilazodone relieved the mechanical allodynia and thermal hyperalgesia induced by CFA in a dose and time-dependent manner (two-way ANOVA and Tukey's test, PWT: $F_{5,42} = 48.32$, $P < 0.0001$, **Fig. 8C**; PWL: $F_{5,42} = 79.02$, $P < 0.0001$, **Fig. 8D**), and repeated vilazodone administration attenuated the mechanical allodynia and thermal hyperalgesia induced by CFA (two-way ANOVA and Tukey's test, $F_{3,28} = 83.5$, $P < 0.0001$, **Fig. 8E**; $F_{3,28} = 40.5$, $P < 0.0001$, **Fig. 8F**; $F_{3,28} = 77.19$, $P < 0.0001$, **Fig. 8G**; $F_{3,28} = 47.13$, $P < 0.0001$, **Fig. 8H**). Importantly, ACE's analgesic effects could be significantly blocked by inhibiting 5-HT_{1A}R activity through repeated administration of WAY-100635 (two-way ANOVA and Tukey's test, $F_{3,28} = 66.8$, $P < 0.0001$, **Fig. 7C**; $F_{3,28} = 29.32$, $P < 0.0001$, **Fig. 7D**; $F_{3,28} = 62.26$, $P < 0.0001$, **Fig. 7E**; $F_{3,28} = 27.21$, $P < 0.0001$, **Fig. 7F**). These results suggest that spinal 5-HT_{1A}R is functionally activated after ACE and that it contributes to the analgesic effects of ACE in CFA-induced inflammatory pain.

Spinal 5-HT_{1A}R activation contributed to ACE analgesia in association with the decreased phosphorylation of the GluN1 subunit of the NMDA receptor

Previous studies have demonstrated that 5-HT_{1A}R activation prevents phosphorylation of GluN1 [37, 54], thus we measured the phosphorylation level of GluN1 after ACE treatment and repeated vilazodone injection. In agreement with previous studies, immunostaining results showed that 5-HT_{1A}R was predominantly co-localized with GluN1 and p-GluN1 in neurons (NeuN, **Fig. 9A-D**), but not in astrocytes (GFAP) or microglial cells (Iba1, **Fig. 9A and B**). Western blotting results showed that the phosphorylation level of GluN1 increased from day 1 to day 15 after CFA injection (one-way ANOVA and Tukey's test, $F = 6.585$, $P = 0.0005$), while no changes were observed in the saline group (one-way ANOVA and Tukey's test, $F = 0.9854$, $P = 0.4470$, **Fig. 9E and F**). Furthermore, the increased phosphorylation of GluN1 was reversed by repeated intrathecal injection of the 5-HT_{1A}R agonist vilazodone or repeated ACE treatment (one-way ANOVA and Tukey's test, day 5: $F= 8.948$, $P < 0.0001$; day 5 CFA+vilazodone vs. CFA: $P = 0.0074$; day 5 CFA+ACE vs. CFA: $P = 0.0267$; day 11: $F = 11.76$, $P < 0.0001$; day 11 CFA+vilazodone vs. CFA: $P = 0.0052$; day 5 CFA+ACE vs. CFA: $P = 0.0021$; **Fig. 9G and H**). Most importantly, the effects of ACE treatment were blocked by repeated intrathecal injection of the 5-HT_{1A}R antagonist WAY-100635 (day 5 CFA+WAY100635+ACE vs. CFA: $P = 0.7908$; day

11 CFA+WAY100635+ACE vs. CFA: P = 0.8051; **Fig. 9G and H**). These findings indicate the involvement of the 5-HT_{1A}R–GluN1 pathway in spinal neurons in mediating the analgesic effects of ACE treatment for inflammatory pain.

Spinal 5-HT_{1A}R activation inhibited the activation of Ca^{2+}-dependent signals

The NMDA receptors play an important role in the regulation of Ca^{2+}-dependent signaling cascades (CaMKII, ERK, and CREB) [29, 49], thus we measured the phosphorylation level of the Ca^{2+}-dependent signaling cascade after ACE treatment and repeated vilazodone injection. Western blotting results showed that the phosphorylation levels of CaMKII (one-way ANOVA and Tukey's test, F = 31.16, P < 0.0001), ERK (one-way ANOVA and Tukey's test, F = 9.793, P < 0.0001), and CREB (one-way ANOVA and Tukey's test, F = 8.367, P = 0.0001) increased from day 1 to day 15 after CFA injection without significant changes in the saline group (one-way ANOVA and Tukey's test, p-CaMKII: F = 1.037, P = 0.419; p-ERK: F = 1.379, P = 0.2672; p-CREB: F = 0.707, P = 0.6238; **Fig. 10A and B**). ACE and repeated vilazodone injection decreased the phosphorylation of CaMKII (day5 CFA+ACE vs. CFA: P = 0.0063; day5 CFA+vilazodone vs. CFA: P < 0.0001; day 11 CFA+ACE vs. CFA: P = 0.0325; day 11 CFA+vilazodone vs. CFA: P = 0.0050), ERK (one-way ANOVA and Tukey's test, day5 CFA+ACE vs. CFA: P = 0.047; day5 CFA+vilazodone vs. CFA: P = 0.0094; day 11 CFA+ACE vs. CFA: P = 0.0128; day 11 CFA+vilazodone vs. CFA: P = 0.0019), and CREB (day5 CFA+ACE vs. CFA: P = 0.012; day5 CFA+vilazodone vs. CFA: P < 0.0001; day 11 CFA+ACE vs. CFA: P = 0.0066; day 11 CFA+vilazodone vs. CFA: P = 0.0017), and the effects of ACE were blocked by repeated WAY-100635 injection (p-CaMKII-day 5 CFA+WAY100635+ACE vs. CFA: P = 0.0758; p-CaMKII-day 11 CFA+WAY100635+ACE vs. CFA: P = 0.5628; p-ERK-day 5 CFA+WAY100635+ACE vs. CFA: P = 0.9630; p-ERK-day 11 CFA+WAY100635+ACE vs. CFA: P = 0.5945; p-CREB-day 5 CFA+WAY100635+ACE vs. CFA: P = 0.1995; p-CREB-day 5 CFA+WAY100635+ACE vs. CFA: P = 0.9874; **Fig. 10C–F**). These results demonstrate that ACE attenuates CFA-induced inflammatory pain at least partially through activation of 5-HT_{1A}R, which inhibits the activation of GluN1 and subsequently decreases the phosphorylation level of Ca^{2+}-dependent signaling pathway proteins.

Discussion

In the current study, we showed that ACE treatments, which were preformed at different frequencies and different acupoints, attenuated the nocifensive response induced by CFA injection. Of all the ACE treatments, it was the best analgesic strategy to inject catgut at the ipsilateral ST36 and GB30 acupoints once a week. Although ACE and EA treatments showed different modes of action, they had similar analgesic effects in our CFA rat model. Mechanistically, ACE inhibited the increased activation of the GluN1 subunit of the NMDA receptor, which in turn decreased the activity of Ca2+-dependent signals (CaMKII, ERK, and CREB) after CFA. Importantly, these effects of ACE were blocked by intrathecal WAY-100635 (a 5-HT_{1A}R antagonist) and could be mimicked by intrathecal vilazodone (a 5-HT_{1A}R agonist). The results of the behavioral tests indicate that ACE is a promising treatment for inflammatory pain and is easier to perform and requires less treatment frequency than EA. In addition, the results of the mechanistic studies suggest that spinal 5-HT_{1A}R–GluN1–Ca^{2+}-dependent signaling might be considered in the development of new pain-relieving therapeutics.

The CFA-induced inflammatory pain rat model was established to imitate clinical inflammatory pain, and the relatively stable time frame was 1–15 days after CFA injection. ACE treatments were performed during this time frame. ACE showed prolonged analgesic effects in this animal model, which is consistent with a recent study [11], and gait analysis showed that ACE ameliorated the abnormal gait induced by CFA injection. It should be noted that the inflamed paws have larger areas after inflammation than the control group. However due to pain, the inflamed paw touched the glass plate only partly and gently, so the mean contact area and the max contact area were not significantly different between the CFA and the control groups. This was consistent with a previous study indicating that the max contact area and mean contact area of mice significantly decreased on day 1–3 after CFA injection, but showed no difference between CFA and naïve groups on day 4–10 after CFA injection[39]. The durations of the stand phase and swing phase are closely related to pain and protective behavior in CFA rats, and these parameters indirectly reflect the pain status of rats. The increased stand phase and decreased swing phase after ACE supports the analgesic role of ACE in CFA-induced inflammatory pain. In our preliminary experiments, the analgesic effects of ACE were studied in two kinds of neuropathic pain models. A weak analgesic effect was observed in a CCI model, but no effect was seen in SNI models (**Fig S4 and Fig S5**), indicating a specific effect of ACE in treating inflammatory pain but not

neuropathic pain in animal models.

To support the clinical application of ACE, the appropriate interval between two treatments, whether one side or two sides is better, and the choice of acupoint compatibility need to be investigated and confirmed. To address these issues, we compared treatment frequency (once a week or once every 4 days), different sides of the rats (ipsilateral, contralateral, or bilateral), and different acupoint compatibility (ST36 alone, GB30 alone, ST36 combined with GB30, or ST25 combined with GB25). We found that ACE at ipsilateral ST36 combined with GB30 acupoints once a week was the least invasive and the most effective. The specificity of acupoints should be noted, although the underlying mechanism for such specificity is unclear. One possible explanation might be that the ST36 and GB30 acupoints are near the knee, with plenty of sciatic nerve endings in the immediate vicinity. Stimulating these points could transmit signals along nerve endings to the central nervous system and thus activate the descending inhibitory modulation.

ACE and EA both involve acupoint stimulation and thus might share some common mechanisms, although the effects of ACE on the sensory nerves might be milder and more gradual. Peripheral stimulation might activate the sensory nervous system through peripheral nerve fibers such as C fibers or A_{δ} fibers, in turn transmitting sensory input to the central nerve system, which triggers the descending inhibitory pathway to the spinal level to intercept the pain signal [56]. Previous studies showed that the endogenous 5-HT (a neurotransmitter associated with pain, body temperature and sleep regulation) descending inhibitory system plays an important role in the modulation of nociceptive transmission by acting on spinal 5-HT_{1A}R [25, 36, 53], and it has been proposed that EA increases the content of 5-HT in the nucleus raphe magnus and the spinal cord [57]. The increased 5-HT acts on spinal 5-HT_{1A}R to alleviate hyperalgesia [53], and the analgesic effects of EA can be blocked by the selective 5-HT_{1A}R antagonist WAY-100635 [54]. Moreover, the 5-HT_{1A}R agonist 8-OH-DPAT attenuates the allodynia induced by carrageenan inflammation [25]. Thus, due to the similarities between the effects of EA and ACE, we studied the role of spinal 5-HT_{1A}R activation in ACE analgesia. Vilazodone, a selective serotonin reuptake inhibitor and a 5-HT_{1A}R partial agonist [15], is approved in the US for the treatment of major depressive disorder in adults, and the effects of vilazodone on rodent anxiety-like behavior were investigated in previous studies [1, 10]. Chronic pain leads to varying severities and qualities of negative affects, such as

anxiety and depression, and these negative affective states in turn enhance pain perception [35]. However, the analgesic effects of vilazodone have not been investigated in animal models. In the present study, vilazodone (100 μg, intrathecal) attenuated the pain induced by CFA in a dose- and time-dependent manner. The analgesic effect of ACE was blocked by the 5-HT_{1A}R antagonist WAY-100635 (30 μg, intrathecal), and taken together these findings support our hypothesis that 5-HT_{1A}R is involved in the analgesic effects of ACE and that this same mechanism is at work with both EA and ACE. However, given that both vilazodone and WAY-100635 were intrathecally injected, the effects of peripheral dorsal root ganglion 5-HT_{1A}R cannot be completely excluded.

The phosphorylation of the GluN1 subunit of the NMDA receptor is known to modulate NMDA receptor activity and to facilitate the transmission of nociceptive inputs in both inflammatory and neuropathic pain models [52]. A previous study showed that 5-HT_{1A}R activation prevents the phosphorylation of the GluN1 subunit [37] and that serotonin depletion increases nociception-evoked trigeminal NMDA receptor phosphorylation [32]. Our immunohistochemistry data showed that 5-HT_{1A}R was predominantly co-localized with GluN1 and p-GluN1 in neurons in the spinal cord, which indicated a functional relationship between 5-HT_{1A}R and the NMDA receptor GluN1 subunit in spinal neurons. Western blot results indicated that ACE inhibited the increase in GluN1 phosphorylation induced by inflammatory pain, which was similar to the effect of the 5-HT_{1A}R agonist vilazodone, and that this effect was blocked by the 5-HT_{1A}R antagonist WAY-100635. These results suggest that 5-HT_{1A}R activation contributes to the analgesia of ACE by inhibiting the phosphorylation of the spinal NMDA receptor GluN1 subunit.

The activation of NMDA receptors induces Ca^{2+} influx, which activates calcium sensors such as CaMKII [58]. These proteins can phosphorylate downstream molecules such as ERK and CREB, which in turn leads to further activation of NMDA receptors and the prolonged enhancement of the excitability of spinal cord neurons [22, 30]. Thus, the Ca^{2+}-dependent signaling molecules (including CaMKII, ERK, and CREB) are regarded as biomarkers for neuronal activation, and they are rapidly activated after exposure to noxious stimuli. The persistent activation of neurons leads to a change of neural plasticity and induces central sensitization [48], which is crucial for the development and maintenance of chronic inflammatory pain [20]. Our western blot results confirmed that the phosphorylation of GluN1 and subsequent Ca^{2+}-dependent signals increase after CFA injection. This increase was inhibited by ACE and vilazodone, and the inhibitory action of ACE

was blocked by WAY-100635. Thus, 5-HT_{1A}R activation might alleviate central sensitization by inhibiting the activation of spinal cord neurons and thus contribute to the analgesic effects of ACE.

It should be taken into account that the analgesic effects of ACE might employ other mechanisms besides the 5-HT_{1A}R-related pathway. In the periphery, 5-HT acts as one of the mediators of neurogenic inflammation and is actively released by platelets, immune cells, and mast cells [41]. The increase of peripheral 5-HT initiates the activation and maintenance of mechanical hypersensitivity, which leads to subsequent sensitization of central neurons [6], and it evokes thermal hyperalgesia [38]. Interestingly, this is in contrast to the function of central 5-HT [53, 57], and thus it was interesting to determine whether peripheral 5-HT is involved in the analgesic effects of ACE. It has been reported that pro-inflammatory molecules contribute to the generation and development of inflammatory pain [9, 40], therefore the inhibition of inflammatory mediator release in response to the catgut stimulation might also be involved in the analgesic effects of ACE. Previous animal studies demonstrated that ACE attenuates airway inflammation and cerebral ischemia-reperfusion injury by inhibiting the expression of NF-κB, TNF-α, and IL-6 [8, 27], and a clinical study indicated that ACE inhibits the expression of IL-6 in patients with acute cerebral infarction [17]. In addition, Du et al. reported that the inhibition of Sigma-1 receptor/p38 mitogen-activating kinase (MAPK) signaling is involved in the analgesic effect of ACE in a CFA model [11]. Previous studies have shown that the activation of p38 MAPK promotes the activation of microglia and the subsequent production and release of proinflammatory factors, such as TNF-α, IL-6, etc., in inflammatory and neuropathic pain[5, 12, 16, 24, 44]. In the present study, ACE showed significant anti-edema effects in the CFA models (**Fig. S2**), which is consistent with Du's work [11]. Thus, it is reasonable to speculate that the analgesic and anti-inflammatory effects effect of ACE were through inhibiting the activation of spinal p38 MAPK and the subsequent release of proinflammatory factors from microglia.

Conclusion

Our present study demonstrates that ACE has a long-lasting analgesic effect on CFA-induced inflammatory pain in rats, which is similar to the effect of EA. However, compared with EA, ACE exerts its effects with significantly reduced treatment frequency and has a non-immediate effect.

Our mechanistic studies indicate that spinal 5-HT_{1A}R activation contributes to the analgesic effect of ACE by inhibiting the activation of the GluN1 subunit of the NMDA receptor and decreasing the subsequent phosphorylation of the Ca^{2+}-dependent signaling molecules CaMKII, ERK, and CREB (**Fig. 10G**). Therefore, ACE might be an effective and convenient treatment option for patients with inflammatory pain.

Authors' contributions

Study design/planning: W.-S. S., Y.-Q. W., Y.-X. C., W.-Q. C., X.-M. H., W.-W. Z.

Study conduct: W.-Q. C., F. X., X.-M. H., Y. Z., L.-X. D., W. Y.

Technical guidance: W.-S. S.

Data analysis: W.-Q. C., F. X., X.-M. H.

Writing paper: W.-Q. C., Y.-Q. W., Y.-X. C, W.-S. S., F. X., X.-M. H., W.-W. Z

Revising paper: all authors

Declaration of interest

The authors declare no competing interests.

Acknowledgements

This study was financially supported by the National Key R&D Program of China (2017YFB0403803), the National Natural Science Funds of China (31600852, 81473749, 81771202), and the Development Project of Shanghai Peak Disciplines-Integrated Chinese and Western Medicine.

References:

1. Adamec R, Bartoszyk GD, Burton P: Effects of systemic injections of vilazodone, a selective serotonin reuptake inhibitor and serotonin 1A receptor agonist, on anxiety induced by predator stress in rats. Eur J Pharmacol. 504:65-77, 2004

2. Baek YH, Choi DY, Yang HI, Park DS: Analgesic effect of electroacupuncture on inflammatory pain in the rat model of collagen-induced arthritis: mediation by cholinergic and serotonergic receptors. Brain Res. 1057:181-185, 2005

3. Berman BM, Lao L, Langenberg P, Lee WL, Gilpin AM, Hochberg MC: Effectiveness of acupuncture as adjunctive therapy in osteoarthritis of the knee: a randomized, controlled trial. Ann Intern Med. 141:901-910, 2004

4. Berman BM, Singh BB, Lao L, Langenberg P, Li H, Hadhazy V, Bareta J, Hochberg M: A randomized trial of acupuncture as an adjunctive therapy in osteoarthritis of the knee. Rheumatology (Oxford). 38:346-354, 1999

5. Berta T, Qadri YJ, Chen G, Ji RR: Microglial Signaling in Chronic Pain with a Special Focus on Caspase 6, p38 MAP Kinase, and Sex Dependence. J Dent Res. 95:1124-1131, 2016

6. Burstein R, Yamamura H, Malick A, Strassman AM: Chemical stimulation of the intracranial dura induces enhanced responses to facial stimulation in brain stem trigeminal neurons. J Neurophysiol. 79:964-982, 1998

7. Cruz CD, Neto FL, Castro-Lopes J, McMahon SB, Cruz F: Inhibition of ERK phosphorylation decreases nociceptive behaviour in monoarthritic rats. Pain. 116:411-419, 2005

8. Cui J, Chen PB, Yang XF, Huang H: [Effect of the simple acupoint catgut embedding on the expression of ICAM-1, NF-kappaB and airway inflammation in rats with asthma]. Zhongguo Zhen Jiu. 30:141-145, 2010

9. Dai T, Shi K, Chen G, Shen Y, Pan T: Malvidin attenuates pain and inflammation in rats with osteoarthritis by suppressing NF-kappaB signaling pathway. Inflamm Res. 66:1075-1084, 2017

10. Dawson LA, Watson JM: Vilazodone: a 5-HT1A receptor agonist/serotonin transporter inhibitor for the treatment of affective disorders. Cns Neurosci Ther. 15:107-117, 2009

11. Du K, Wang X, Chi L, Li W: Role of Sigma-1 Receptor/p38 MAPK Inhibition in Acupoint Catgut Embedding-Mediated Analgesic Effects in Complete Freund's Adjuvant-Induced Inflammatory Pain. Anesth Analg. 125:662-669, 2017

12. Fang JQ, Du JY, Liang Y, Fang JF: Intervention of electroacupuncture on spinal p38 MAPK/ATF-2/VR-1 pathway in treating inflammatory pain induced by CFA in rats. Mol Pain. 9:13, 2013

13. Feng Y: [Clinical effect on migraine treated with acupoint implantation]. Zhongguo Zhen Jiu. 36:373-375, 2016

14. Ferland CE, Laverty S, Beaudry F, Vachon P: Gait analysis and pain response of two rodent models of osteoarthritis. Pharmacol Biochem Behav. 97:603-610, 2011

15. Gommoll C, Durgam S, Mathews M, Forero G, Nunez R, Tang X, Thase ME: A double-blind, randomized, placebo-controlled, fixed-dose phase III study of vilazodone in patients with generalized anxiety disorder. Depress Anxiety. 32:451-459, 2015

16. Gu W, Wang Y, Qiu Z, Dong J, Wang Y, Chen J: Mitogen-activated protein kinase signaling is involved in nonylphenol-induced proinflammatory cytokines secretion by BV2 microglia. J Appl Toxicol. 38:958-967, 2018

17. Guo AS, Li AH, Chen X, Chen WG, Sun L: [Effect of acupoint catgut embedding on motor function and serum high sensitivity C-reactive protein and IL-6 levels in patients with acute cerebral infarction]. Zhen Ci Yan Jiu. 38:224-228, 258, 2013

18. Guo T, Ren Y, Kou J, Shi J, Tianxiao S, Liang F: Acupoint Catgut Embedding for Obesity: Systematic Review and Meta-Analysis. Evid Based Complement Alternat Med. 2015:401914, 2015

19. Hamers FP, Lankhorst AJ, van Laar TJ, Veldhuis WB, Gispen WH: Automated quantitative gait analysis during overground locomotion in the rat: its application to spinal cord contusion and transection injuries. J Neurotrauma. 18:187-201, 2001

20. Hanack C, Moroni M, Lima WC, Wende H, Kirchner M, Adelfinger L, Schrenk-Siemens K, Tappe-Theodor A, Wetzel C, Kuich PH, Gassmann M, Roggenkamp D, Bettler B, Lewin GR, Selbach M, Siemens J: GABA blocks pathological but not acute TRPV1 pain signals. Cell. 160:759-770, 2015

21. Hargreaves K, Dubner R, Brown F, Flores C, Joris J: A new and sensitive method for measuring thermal nociception in cutaneous hyperalgesia. Pain. 32:77-88, 1988

22. Hucho T, Levine JD: Signaling pathways in sensitization: toward a nociceptor cell biology. Neuron. 55:365-376, 2007

23. Hylden JL, Wilcox GL: Intrathecal morphine in mice: a new technique. Eur J Pharmacol. 67:313-316, 1980

24. Ji RR, Suter MR: p38 MAPK, microglial signaling, and neuropathic pain. Mol Pain. 3:33, 2007

25. Kim JM, Jeong SW, Yang J, Lee SH, Kim WM, Jeong S, Bae HB, Yoon MH, Choi JI: Spinal 5-HT1A, not the 5-HT1B or 5-HT3 receptors, mediates descending serotonergic inhibition for late-phase mechanical allodynia of carrageenan-induced peripheral inflammation. Neurosci Lett. 600:91-97, 2015

26. Kim SK, Park JH, Bae SJ, Kim JH, Hwang BG, Min BI, Park DS, Na HS: Effects of electroacupuncture on cold allodynia in a rat model of neuropathic pain: mediation by spinal adrenergic and serotonergic receptors. Exp Neurol. 195:430-436, 2005

27. Kong LH, Sun GJ, Mao JJ, Su FR, Gao S: [Effects of acupoint-embedding of medicinal thread and electroacupuncture on contents of TNF-alpha and IL-6 of hippocampus tissue in rats with focal cerebral ischemia-reperfusion injury]. Zhen Ci Yan Jiu. 32:301-305, 2007

28. Li X, Liu Y, Zhang Q, Xiang N, He M, Zhong J, Chen Q, Wang X: Effect of catgut implantation at acupoints for the treatment of allergic rhinitis: a randomized, sham-controlled trial. BMC Complement Altern Med. 16:454, 2016

29. Liu S, Liu WT, Liu YP, Dong HL, Henkemeyer M, Xiong LZ, Song XJ: Blocking EphB1 receptor forward signaling in spinal cord relieves bone cancer pain and rescues analgesic effect of morphine treatment in rodents. Cancer Res. 71:4392-4402, 2011

30. Liu S, Mi WL, Li Q, Zhang MT, Han P, Hu S, Mao-Ying QL, Wang YQ: Spinal IL-33/ST2 Signaling Contributes to Neuropathic Pain via Neuronal CaMKII-CREB and Astroglial JAK2-STAT3 Cascades in Mice. Anesthesiology. 123:1154-1169, 2015

31. Ma Y, Li X, Li F, Yu W, Wang Z: [Clinical research of chronic pelvic cavity pain syndrome treated with acupoint catgut embedding therapy]. Zhongguo Zhen Jiu. 35:561-566, 2015

32. Maneepak M, le Grand S, Srikiatkhachorn A: Serotonin depletion increases nociception-evoked trigeminal NMDA receptor phosphorylation. Headache. 49:375-382, 2009

33. Mao-Ying QL, Wang XW, Yang CJ, Li X, Mi WL, Wu GC, Wang YQ: Robust spinal neuroinflammation mediates mechanical allodynia in Walker 256 induced bone cancer rats. Mol Brain. 5:16, 2012

34. Melchart D, Weidenhammer W, Streng A, Reitmayr S, Hoppe A, Ernst E, Linde K: Prospective investigation of adverse effects of acupuncture in 97 733 patients. Arch Intern Med. 164:104-105, 2004

35. Rhudy JL, Meagher MW: Fear and anxiety: divergent effects on human pain thresholds. Pain. 84:65-75, 2000

36. Sagalajev B, Bourbia N, Beloushko E, Wei H, Pertovaara A: Bidirectional amygdaloid control of neuropathic hypersensitivity mediated by descending serotonergic pathways acting on spinal 5-HT3 and 5-HT1A receptors. Behav Brain Res. 282:14-24, 2015

37. Salazar-Colocho P, Del RJ, Frechilla D: Serotonin 5-hT1A receptor activation prevents

phosphorylation of NMDA receptor NR1 subunit in cerebral ischemia. J Physiol Biochem. 63:203-211, 2007

38. Sanchez DRM, Reuter U, Moskowitz MA: Central and peripheral mechanisms of migraine. Funct Neurol. 15 Suppl 3:157-162, 2000

39. Shepherd AJ, Mohapatra DP: Pharmacological validation of voluntary gait and mechanical sensitivity assays associated with inflammatory and neuropathic pain in mice. Neuropharmacology. 130:18-29, 2018

40. Singh AK, Vinayak M: Curcumin attenuates CFA induced thermal hyperalgesia by modulation of antioxidant enzymes and down regulation of TNF-alpha, IL-1beta and IL-6. Neurochem Res. 40:463-472, 2015

41. Sommer C: Serotonin in pain and analgesia: actions in the periphery. Mol Neurobiol. 30:117-125, 2004

42. Sun W, Chu N, Feng Y, Wang Y, Ma Y, Jiang G: [Preliminary study on depth of embedded catgut and qi arrival at cervical Jiaji (EX-B 2) under ultrasound guidance]. Zhongguo Zhen Jiu. 35:931-934, 2015

43. Sun W, Chu N, Ma Y, Wang Y, Wang H, Jiang G: [Effective anatomic structures of ultrasound-guide acupoint embedding therapy for cervical spondylosis]. Zhongguo Zhen Jiu. 35:1001-1004, 2015

44. Taves S, Berta T, Liu DL, Gan S, Chen G, Kim YH, Van de Ven T, Laufer S, Ji RR: Spinal inhibition of p38 MAP kinase reduces inflammatory and neuropathic pain in male but not female mice: sex-dependent microglial signaling in the spinal cord. Brain Behav Immun. 55:70-81, 2016

45. Vrinten DH, Hamers FF: 'CatWalk' automated quantitative gait analysis as a novel method to assess mechanical allodynia in the rat; a comparison with von Frey testing. Pain. 102:203-209, 2003

46. Wang K, Ju Z, Yong Y, Chen T, Song J, Zhou J: The Effects of Electroacupuncture on the Apelin/APJ System in the Spinal Cord of Rats With Inflammatory Pain. Anesth Analg. 123:1603-1610, 2016

47. White A, Hayhoe S, Hart A, Ernst E: Survey of adverse events following acupuncture (SAFA): a prospective study of 32,000 consultations. Acupunct Med. 19:84-92, 2001

48. Woolf CJ, Salter MW: Neuronal plasticity: increasing the gain in pain. Science. 288:1765-1769, 2000

49. Wu XF, Liu WT, Liu YP, Huang ZJ, Zhang YK, Song XJ: Reopening of ATP-sensitive potassium channels reduces neuropathic pain and regulates astroglial gap junctions in the rat spinal cord. Pain. 152:2605-2615, 2011

50. Yamashita H, Tsukayama H, Hori N, Kimura T, Tanno Y: Incidence of adverse reactions associated with acupuncture. J Altern Complement Med. 6:345-350, 2000

51. Yang CH: [Forty cases of scapulohumeral periarthritis treated by catgut embedding at Qiangji (extra) and local points]. Zhongguo Zhen Jiu. 33:938, 2013

52. Zhang X, Wu J, Lei Y, Fang L, Willis WD: Protein phosphatase modulates the phosphorylation of spinal cord NMDA receptors in rats following intradermal injection of capsaicin. Brain Res Mol Brain Res. 138:264-272, 2005

53. Zhang Y, Li A, Xin J, Lao L, Ren K, Berman BM, Tan M, Zhang RX: Involvement of spinal serotonin receptors in electroacupuncture anti-hyperalgesia in an inflammatory pain rat model. Neurochem Res. 36:1785-1792, 2011

54. Zhang Y, Zhang RX, Zhang M, Shen XY, Li A, Xin J, Ren K, Berman BM, Tan M, Lao L:

Electroacupuncture inhibition of hyperalgesia in an inflammatory pain rat model: involvement of distinct spinal serotonin and norepinephrine receptor subtypes. Br J Anaesth. 109:245-252, 2012

55. Zhang YJ, Cao HJ, Li XL, Yang XY, Lai BY, Yang GY, Liu JP: Cupping therapy versus acupuncture for pain-related conditions: a systematic review of randomized controlled trials and trial sequential analysis. Chin Med. 12:21, 2017

56. Zhao L, Cheng K, Wang L, Wu F, Deng H, Tan M, Lao L, Shen X: Effectiveness of moxibustion treatment as adjunctive therapy in osteoarthritis of the knee: a randomized, double-blinded, placebo-controlled clinical trial. Arthritis Res Ther. 16:R133, 2014

57. Zhao ZQ: Neural mechanism underlying acupuncture analgesia. Prog Neurobiol. 85:355-375, 2008

58. Zhuo M, Wu G, Wu LJ: Neuronal and microglial mechanisms of neuropathic pain. Mol Brain. 4:31, 2011

59. Zimmermann M: Ethical guidelines for investigations of experimental pain in conscious animals. Pain. 16:109-110, 1983

Figure legends

Fig. 1. The needle **(A)**, catgut **(B)**, and schematic **(C)** of ACE.

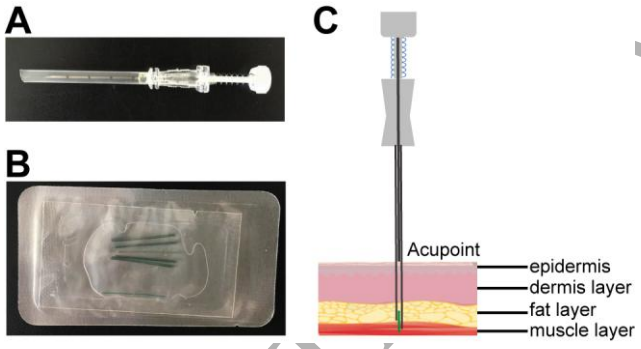

Fig. 2. The rat model of inflammatory pain was established by intraplantar injection of CFA. The time course of changes in PWT in response to von Frey filament stimuli **(A)** and changes in PWLs in response to radiant heat **(B)**. **P* < 0.05, ****P* < 0.001 compared with the naive group; n = 8 rats for each group.

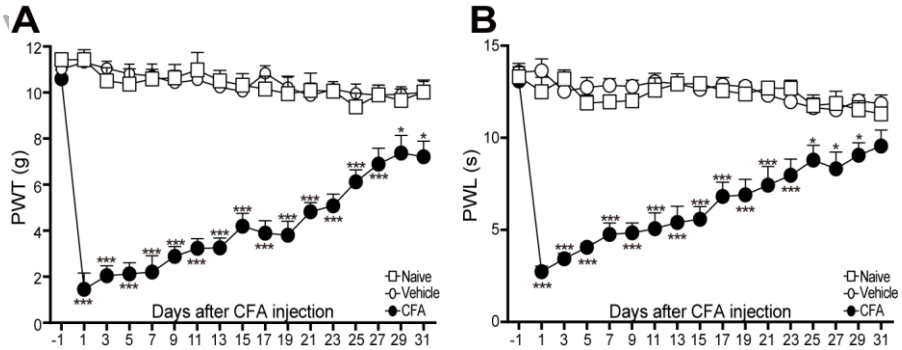

Fig. 3. The analgesic effects of ACE at different frequencies and different sides of the rats on

CFA-induced inflammatory pain. ACE performed at the ipsilateral, contralateral, or bilateral ST36 and GB30 acupoints at a frequency of once a week (two hours after the behavior tests on day 1 and 8 after CFA injection) or once every 4 days (two hours after the behavior tests on day 1, 5, 9, and 13 after CFA injection) significantly reversed the decreased PWTs and PWLs induced by CFA application compared with the CFA control group (**A–C, G–H**). No significant difference in PWTs was seen when ACE was applied once a week after CFA injection compared with every 4 days at contralateral (**A**), ipsilateral (**B**), and bilateral (**C**) acupoints ($P > 0.05$ for all). At the frequency of once a week, bilateral ACE showed better analgesic effects compared with contralateral ACE (**D**, $P < 0.05$), whereas the PWTs in the ipsilateral ACE group showed no significant difference compared with bilateral ACE (**E**, $P > 0.05$) or contralateral ACE (**F**, $P > 0.05$). The PWLs showed no difference when ACE was performed weekly on the ipsilateral side compared with every 4 days on the ipsilateral side (**G**, $P > 0.05$) or weekly on the bilateral sides (**H**, $P > 0.05$). *$P < 0.05$, **$P < 0.01$, ***$P < 0.001$ compared with the CFA group, n = 8 rats for each group. The arrows indicate the treatment time points. All data are shown as the mean ± SEM. contra. = contralateral, ipsi. = ipsilateral, bi. = bilateral, 1/4D = once every four days, 1/W = once a week.

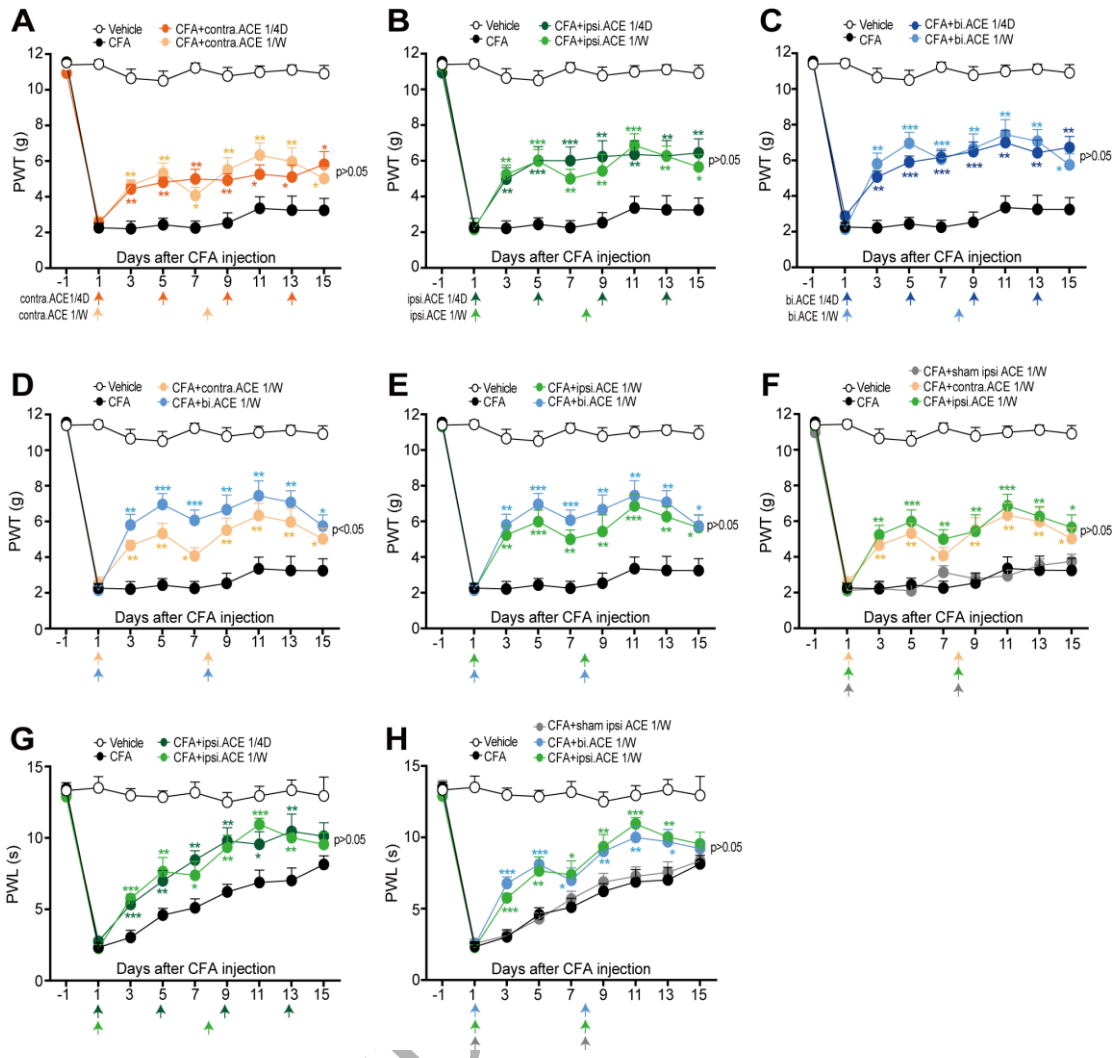

Fig. 4. The analgesic effects of ACE at different acupoints on CFA-induced inflammatory pain. **(A)** Ipsilateral ACE (two hours after the behavior tests on day 1 and 8 after CFA injection) performed at ST36 combined with GB30 at a frequency of once per week significantly reversed the decreased PWTs induced by CFA injection compared to ACE at GB30 alone ($P < 0.05$), ST36 alone ($P < 0.05$), or ST25 combined with GB25 ($P < 0.05$). **(B)** The decreased PWLs after CFA injection were significantly reversed in ipsilateral ACE application at ST36 combined with GB30 at a frequency of once per week compared with GB30 alone ($P < 0.05$), ST36 alone ($P < 0.05$), or ST25 combined with GB25 ($P < 0.05$). *$P < 0.05$, **$P < 0.01$, ***$P < 0.001$ compared with the CFA group, n = 8 rats for each group. The arrows indicate the treatment time points. All data are shown as the mean ± SEM.

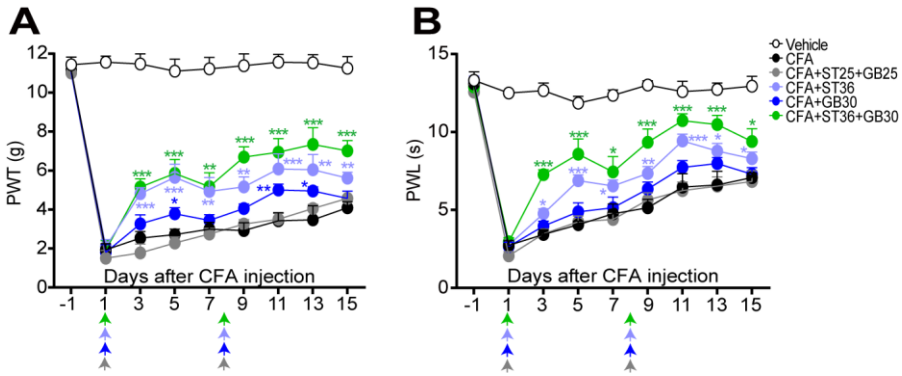

Fig. 5. The effects of ipsilateral ACE (at ST36 combined with GB30) on gait behavior in CFA-induced inflammatory pain. The print view and timing view of the right hind paw (RH) and left hind paw (LH) when the rats walked across the device at day 5 **(A)** and day 11 **(B)** after CFA (4 days after the first ACE treatment and 3 days after second ACE treatment, respectively). The max contact area **(C)** and mean contact area **(D)** of the ipsilateral hind paw (as measured by the RH/LH ratio) had no significant changes after CFA and ACE at day 5 or day 11 post-CFA. ACE increased the max contact max intensity **(E)** and mean intensity **(F)** of the ipsilateral hind paw at day 5 and day 11 after CFA. The stand **(G)** and swing **(H)** phases of the rats at day 5 and day 11 after CFA. $*P < 0.05$, $**P < 0.01$, $***P < 0.001$; n = 8 rats for each group. All data are shown as the mean ± SEM.

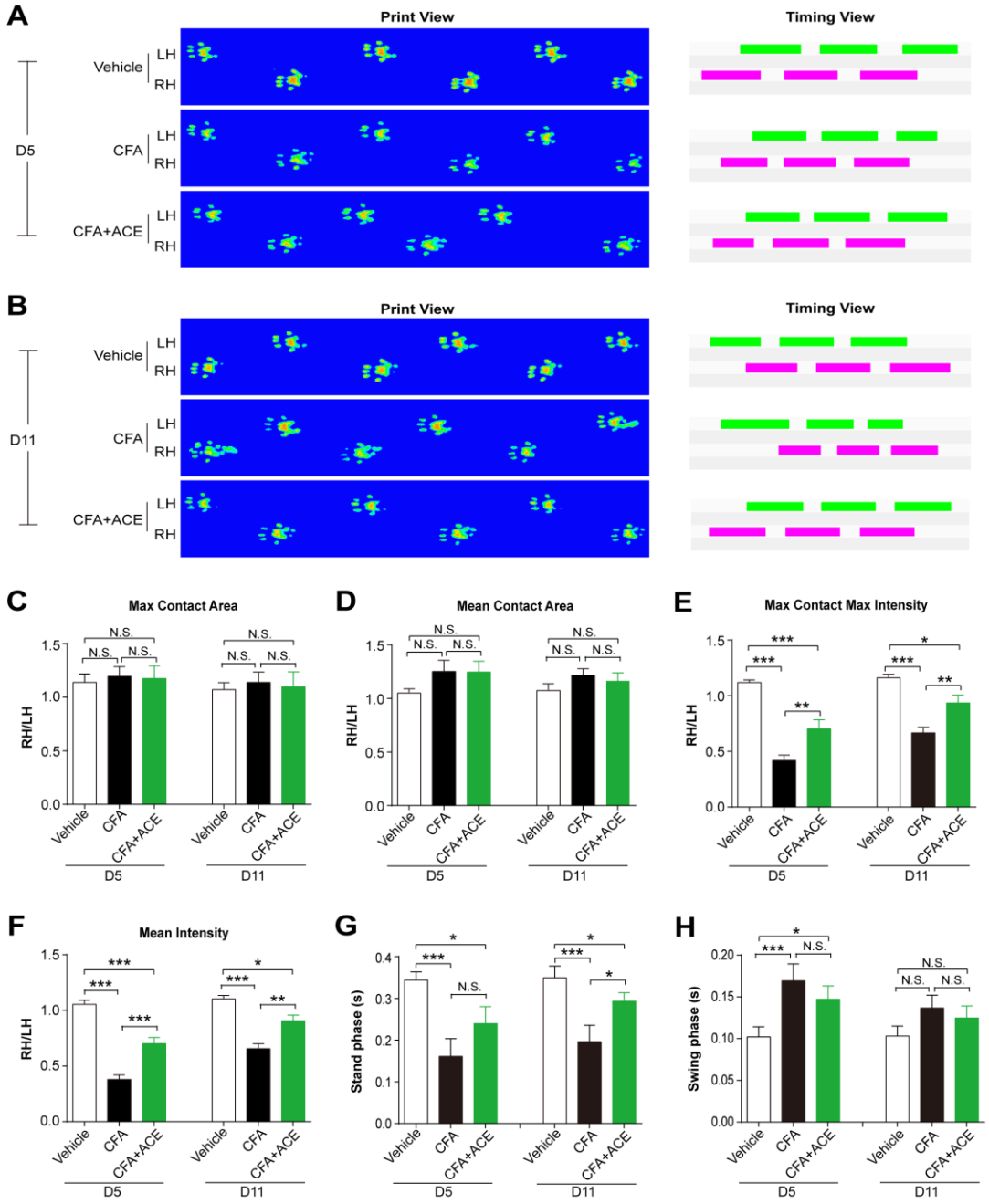

Fig. 6. The effects of ACE and EA at ipsilateral ST36 combined with GB30 on CFA-induced inflammatory pain. A single EA treatment showed immediate effects on alleviating mechanical allodynia **(A)** and thermal hyperalgesia **(B)**, while a single ACE treatment did not. In contrast, a single ACE treatment showed analgesic effects that lasted for a few days, while single EA did not **(C and D)**. Repeated ACE (once a week) or EA (every 2 days, performed two hours after the behavior tests on day 1 after CFA injection, and two hours before the behavior tests on other administering days) showed long-lasting analgesic effects in alleviating mechanical allodynia **(E)** and thermal hyperalgesia **(F)** induced by CFA, and there was no significant difference between

these two treatments ($P > 0.05$). *$P < 0.05$, **$P < 0.01$, ***$P < 0.001$ compared with the CFA group; n = 8 rats for each group. The arrows indicate the time points for each treatment. All data are shown as the mean ± SEM.

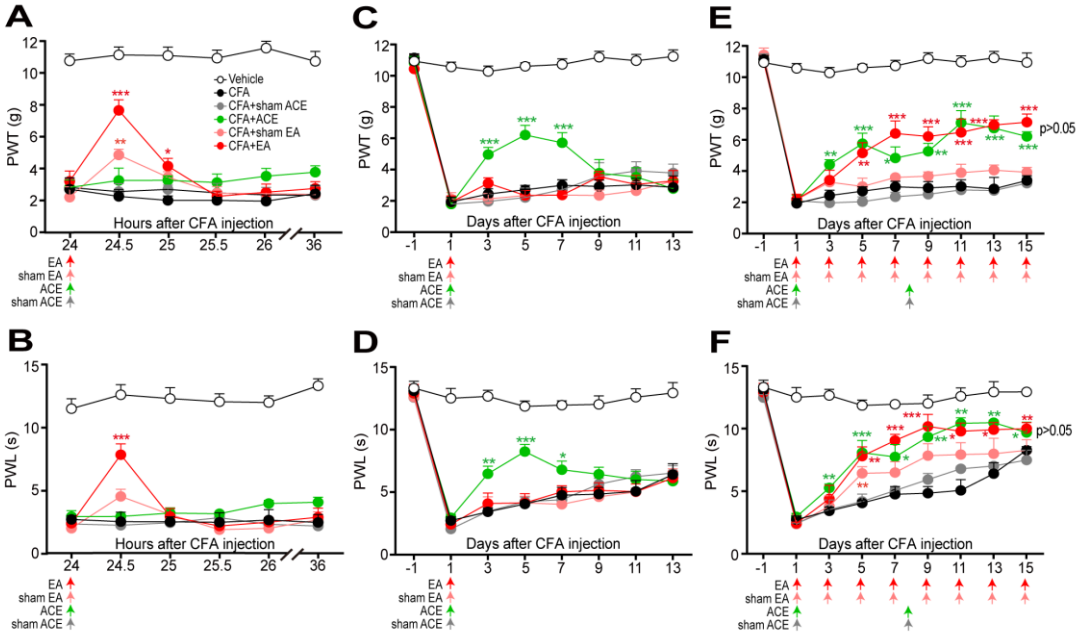

Fig. 7. 5-HT_{1A}R blockade reversed the analgesic effects of ACE on CFA-induced inflammatory pain. The 5-HT_{1A}R selective antagonist (WAY-100635, 30 μg, intrathecal) showed no effects on PWT **(A)** or PWL **(B)** in naïve rats. WAY-100635, which was administered after CFA injection (15 minutes before ACE on day 1 or 8, and half an hour before the behavior tests on day 3 and 5 or day 9 and 11 after CFA injection), reversed the analgesic effects of ACE in terms of both PWT **(C, E)** and PWLs **(D, F)**. *$P < 0.05$, **$P < 0.01$, ***$P < 0.001$ compared with the CFA group; n = 8 rats for each group. The arrows indicate the time points for each treatment. All data are shown as the mean ± SEM.

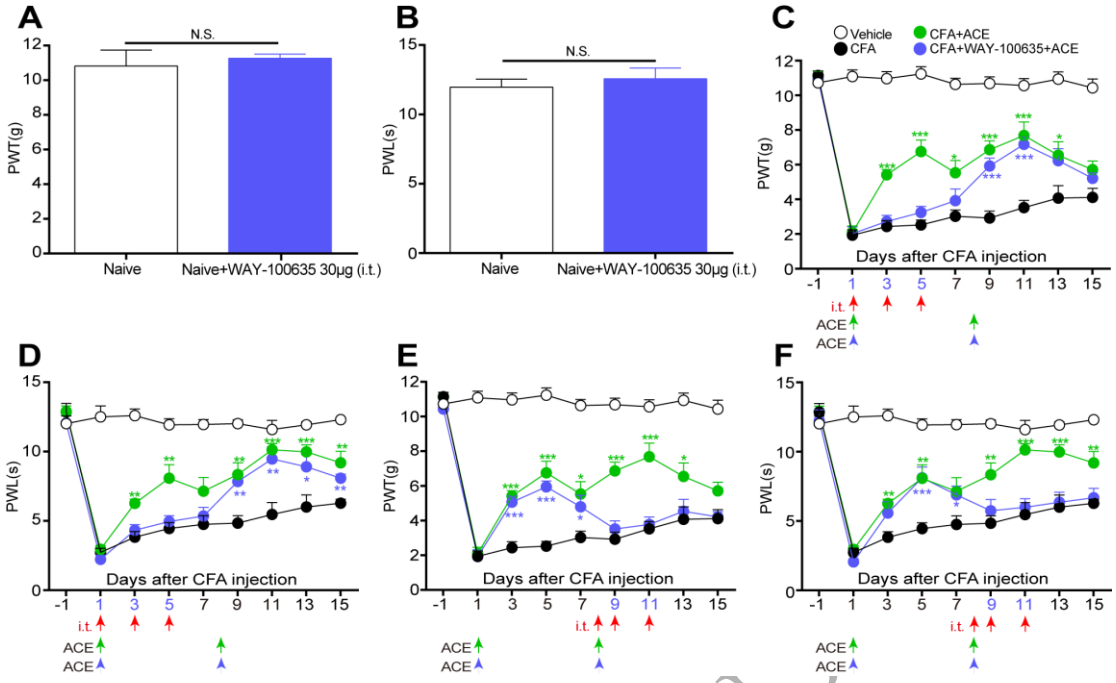

Fig. 8. 5-HT_{1A}R activation attenuated the nocifensive response induced by CFA injection. The 5-HT_{1A}R partial agonist vilazodone (100 μg, intrathecal) showed no effect on the PWT **(A)** or PWL **(B)** in naïve rats. Activation of 5-HT_{1A}R by vilazodone (1 μg, 10 μg, and 100 μg, intrathecal) dose-dependently reversed the decreased PWT **(C)** and PWL **(D)** induced by CFA injection. Vilazodone (100 μg, intrathecal), which was administered (two hours after behavior testing on day 1 or 8, two hours before the behavior tests on day 3 and 5 or day 9 and 11 after CFA injection) after CFA injection rescued the decreased PWT **(E, G)** and PWL **(F, H)**. **P* < 0.05, ***P* < 0.01, ****P* < 0.001 compared with the CFA group; n = 8 rats for each group. The arrows indicate the treatment time points. All data are shown as the mean ± SEM.

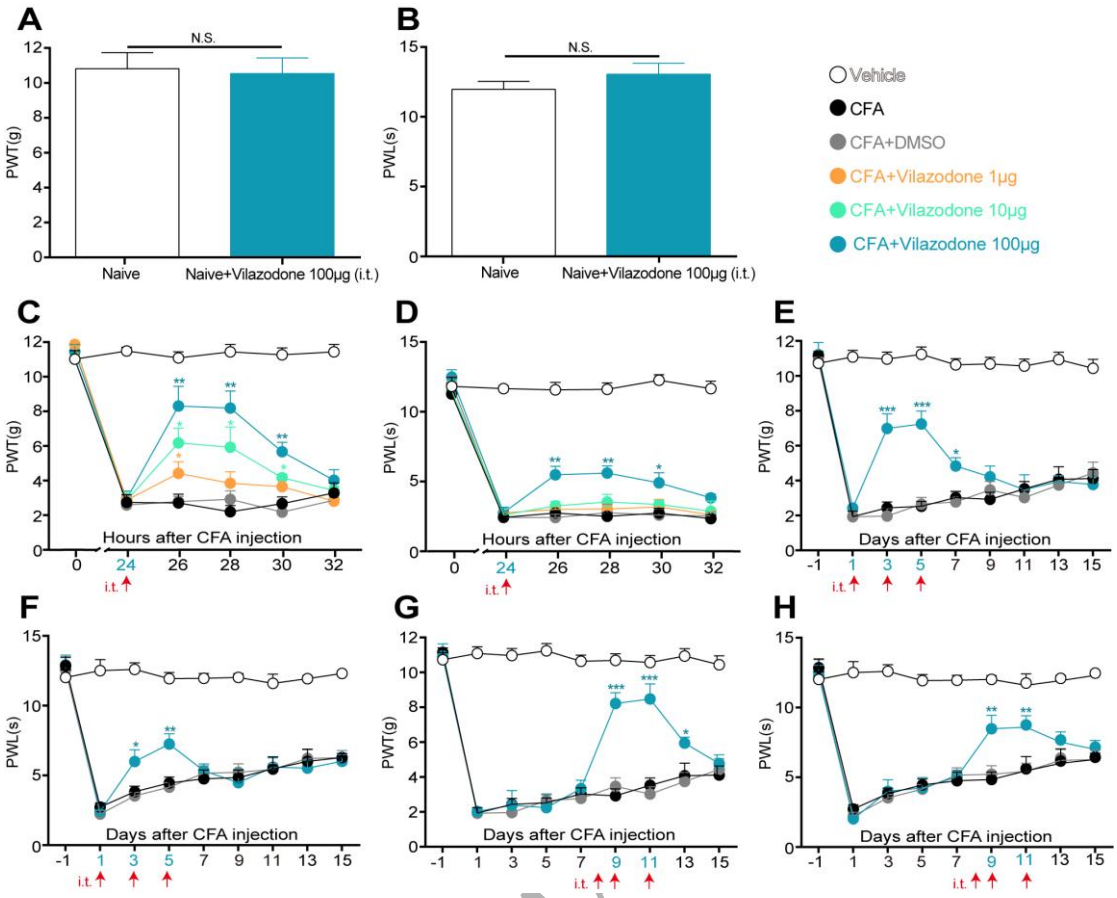

Fig. 9. The role of spinal 5-HT_{1A}R in the regulation of phosphorylated NMDA receptor GluN1 subunit in CFA rats. **(A and B)** 5-HT_{1A}R and GluN1 were co-localized with NeuN (a neuronal marker, top row) but not with GFAP (an astrocyte marker, middle row) or Iba-1 (a microglial marker, bottom row) in the spinal dorsal horn at day 5 after CFA injection. Double immunostaining of 5-HT_{1A}R (green) and GluN1 **(C)** or p-GluN1 **(D)**. Scale bars: 50 μm (left three columns of A–D); 20 μm (right column of A–D). **(E and F)** Western blot analysis showing the time course of the expression of p-GluN1 after CFA. **(G and H)** Western blot analysis showing the changes in p-GluN1 protein expression in each group at day 5 and day 11 after CFA administration. $^{*}P < 0.05$, $^{**}P < 0.01$, $^{***}P < 0.001$ compared with the naïve or sham group; $^{\#}P < 0.05$, $^{\#\#}P < 0.01$ compared with the CFA group. n = 5 rats for each group. All data are shown as the mean ± SEM.

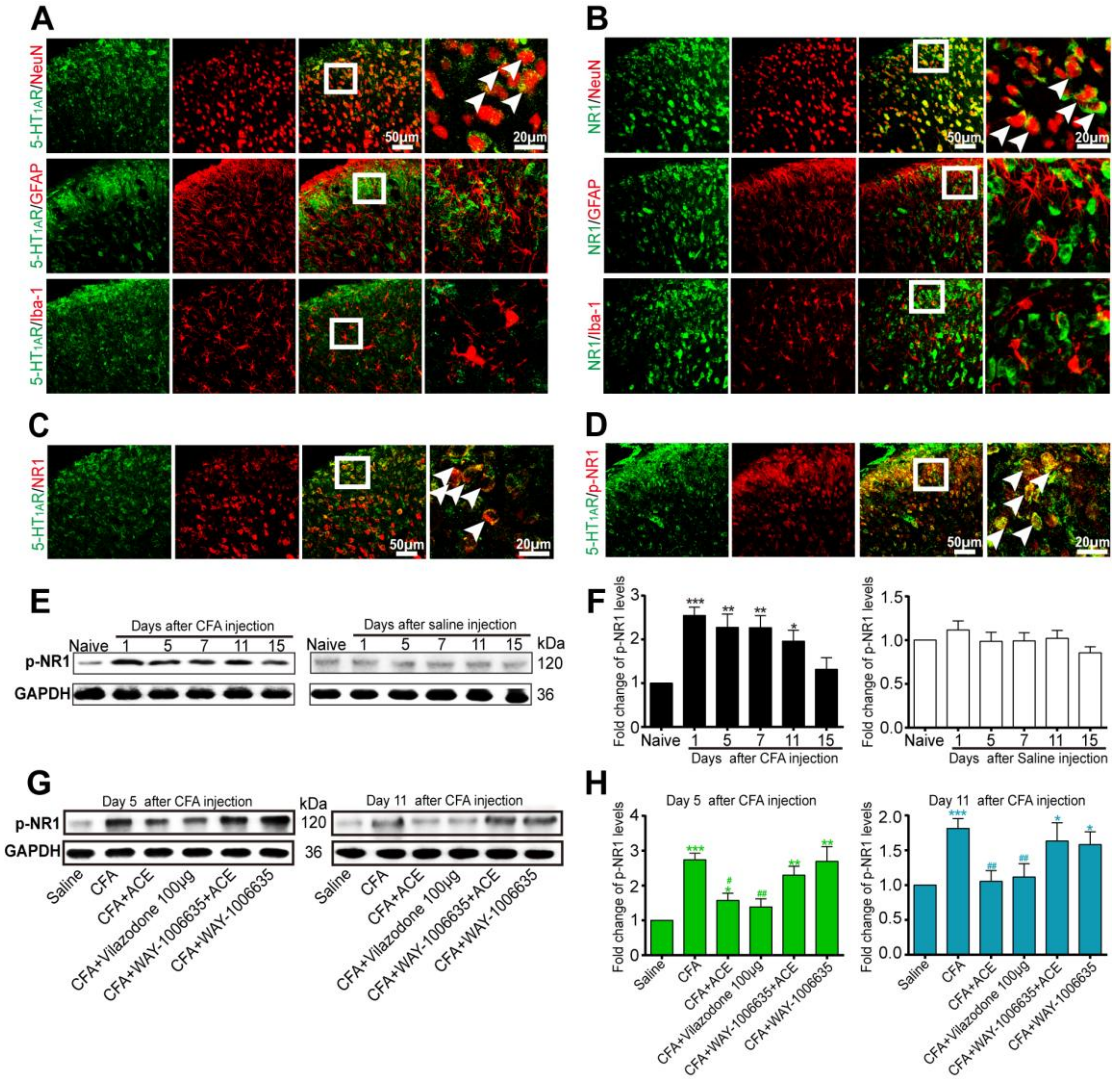

Fig. 10. Role of spinal 5-HT_{1A}R in the regulation of phosphorylated CaMKII, ERK, and CREB in CFA rats. Western blot analysis showing the time course of p-CaMKII, p-ERK, and p-CREB levels after CFA or saline injection **(A and B)** and the changes in p-CaMKII, p-ERK, and p-CREB levels in the ACE, ACE plus WAY-100635, CFA plus vilazodone, and CFA plus WAY-100635 groups at day 5 **(C and D)** and day 11 **(E and F)** after CFA injection. **(G)** A schematic overview of the CaMKII/ERK/CREB pathway activated by GluN1 and that was inhibited by ACE-induced 5-HT_{1A}R activation in spinal neurons. *$P < 0.05$, **$P < 0.01$, ***$P < 0.001$ compared with the naive group; $^{\#}P < 0.05$, $^{\#\#}P < 0.01$, $^{\#\#\#}P < 0.001$ compared with the CFA group, n = 5 rats for each group. All data are shown as the mean ± SEM.